

Supporting Information for

## Plasmonic Ag-Decorated Few-Layer MoS<sub>2</sub> Nanosheets Vertically Grown on Graphene for Efficient Photoelectrochemical Water Splitting

Dong-Bum Seo<sup>1</sup>, Tran Nam Trung<sup>1</sup>, Dong-Ok Kim<sup>1</sup>, Duong Viet Duc<sup>1</sup>, Sungmin Hong<sup>2</sup>, Youngku Sohn<sup>2</sup>, Jong-Ryul Jeong<sup>1</sup>, Eui-Tae Kim<sup>1</sup>, \*

<sup>1</sup>Department of Materials Science & Engineering, Chungnam National University, Daejeon 34134, Republic of Korea

<sup>2</sup>Department of Chemistry, Chungnam National University, Daejeon 34134, Republic of Korea

\*Corresponding author. E-mail: [etkim@cnu.ac.kr](mailto:etkim@cnu.ac.kr) (Eui-Tae Kim)

### Supplementary Figures and Table

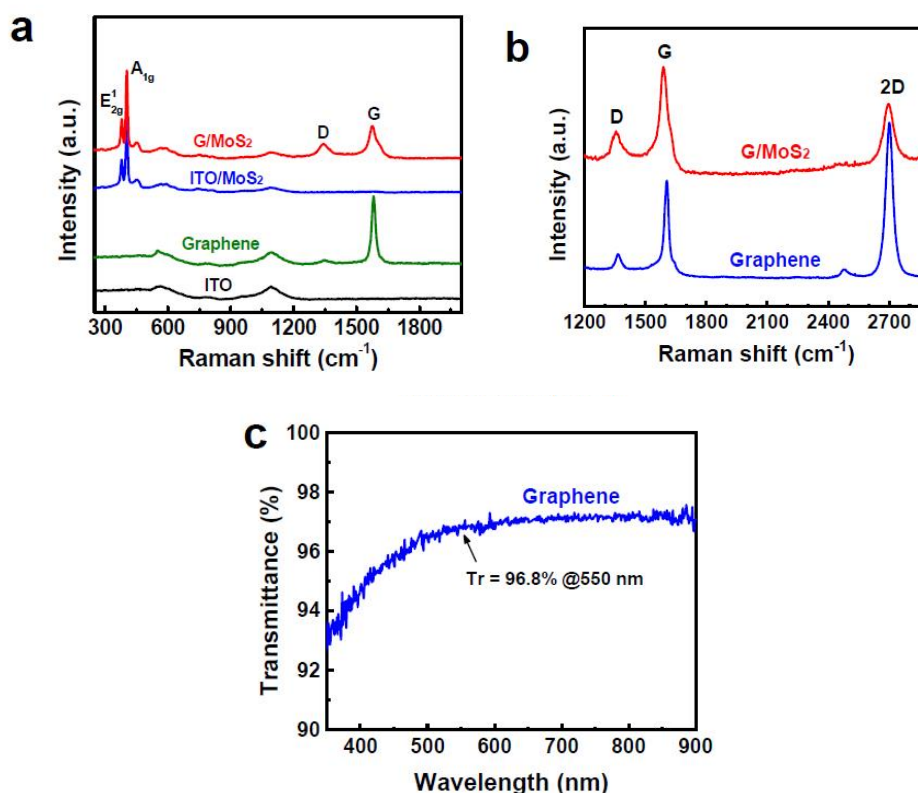


**Fig. S1** (a) Raman spectra of ITO, pristine graphene, ITO/MoS<sub>2</sub>, and G/MoS<sub>2</sub>. (b) Graphene-region Raman spectra of pristine graphene and G/MoS<sub>2</sub>. (c) UV-Vis absorption spectrum of pristine graphene, exhibiting light transmittance of 96.8% at 550 nm

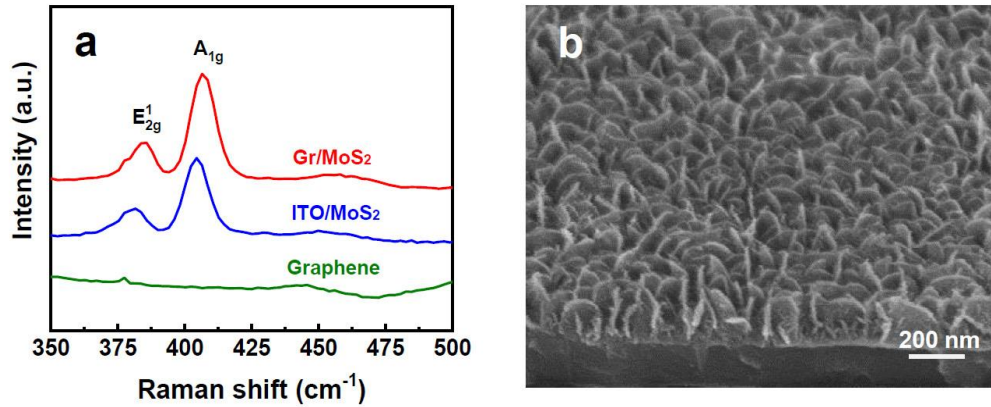


**Fig. S2** (a) Raman spectra of pristine graphene, ITO/MoS<sub>2</sub>, and G/MoS<sub>2</sub>. (b) SEM images of few-layer MoS<sub>2</sub> nanosheets grown on ITO (ITO/MoS<sub>2</sub>)

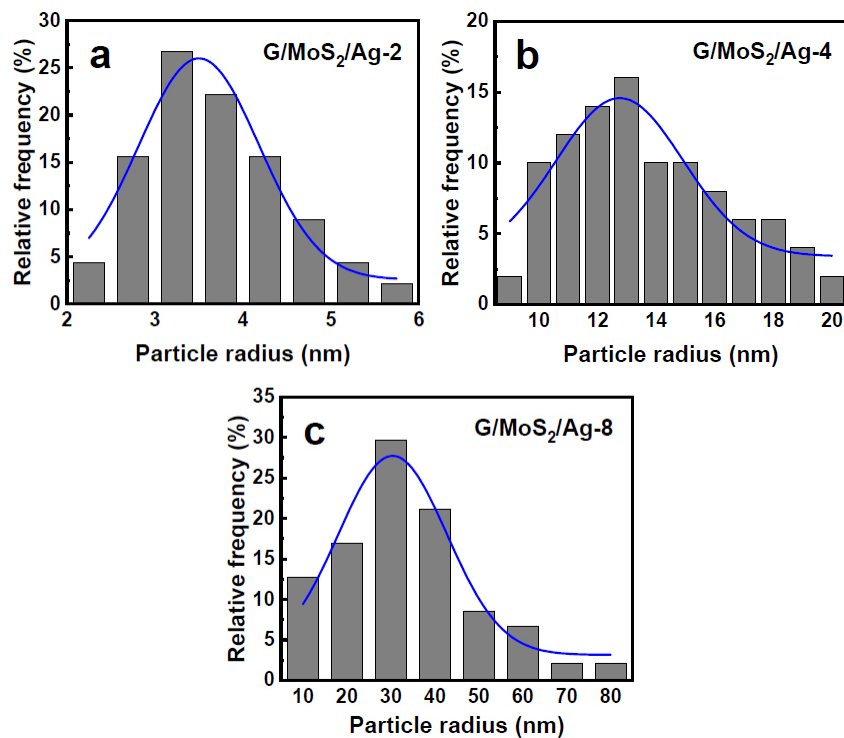


**Fig. S3** Ag NP size distribution of (a) G/MoS<sub>2</sub>/Ag-2, (b) G/MoS<sub>2</sub>/Ag-4, and (c) G/MoS<sub>2</sub>/Ag-8

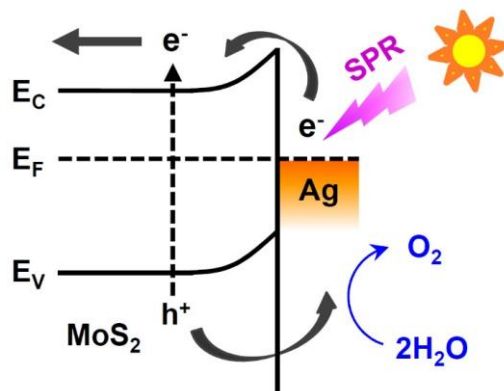


**Fig. S4** Energy band diagram of the Schottky junction of MoS<sub>2</sub>/Ag

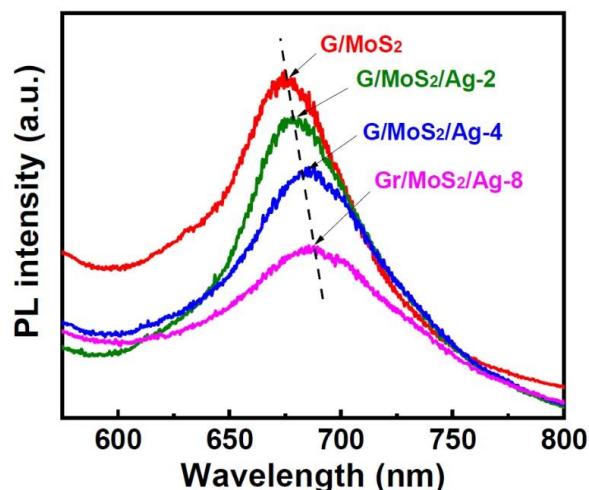


**Fig. S5** PL spectra of G/MoS<sub>2</sub>, G/MoS<sub>2</sub>/Ag-2, G/MoS<sub>2</sub>/Ag-4, and G/MoS<sub>2</sub>/Ag-8

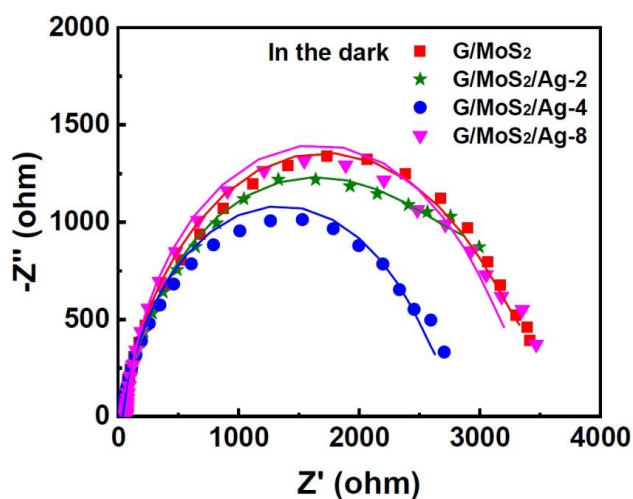


**Fig. S6** Nyquist plots of G/MoS<sub>2</sub>, G/MoS<sub>2</sub>/Ag-2, G/MoS<sub>2</sub>/Ag-4, and G/MoS<sub>2</sub>/Ag-8 in the dark

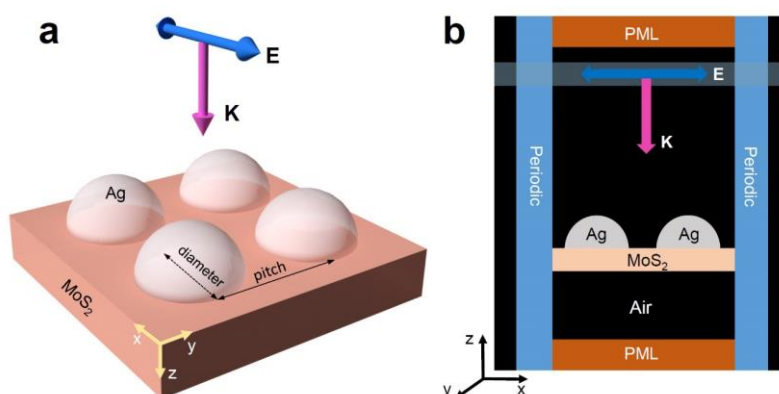


**Fig. S7** (a) Schematic representation of the formulated structure for FDTD simulations. The Ag NPs on a three-layer-thick MoS<sub>2</sub> substrate is irradiated by a plane-wave source with the propagation vector in the  $z$ -direction and the E-field oscillating along the  $x$ -axis. (b) Real simulation environment with applied periodic boundary conditions

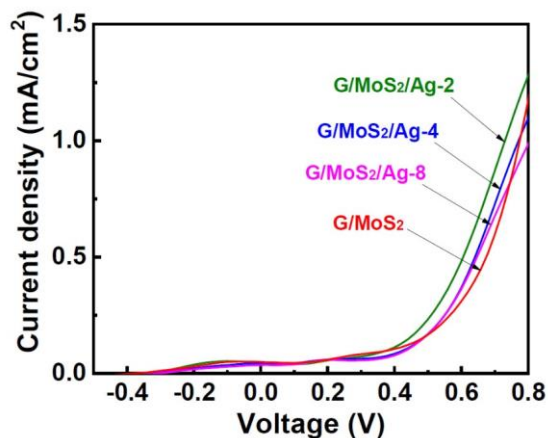


**Fig. S8** Dark current density–potential curves of PEC cells with various working electrodes (G/MoS<sub>2</sub>, G/MoS<sub>2</sub>/Ag-2, G/MoS<sub>2</sub>/Ag-4, and G/MoS<sub>2</sub>/Ag-8)

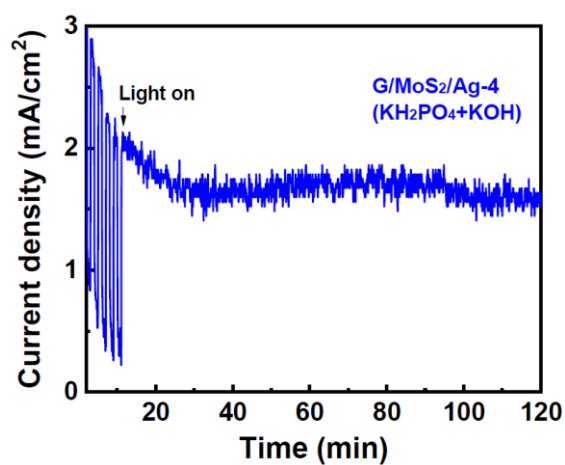


**Fig. S9** Repeated photocurrent–time measurement for G/MoS<sub>2</sub>/Ag-4 in 0.3 M KH<sub>2</sub>PO<sub>4</sub> + 0.3 M KOH solution after a month

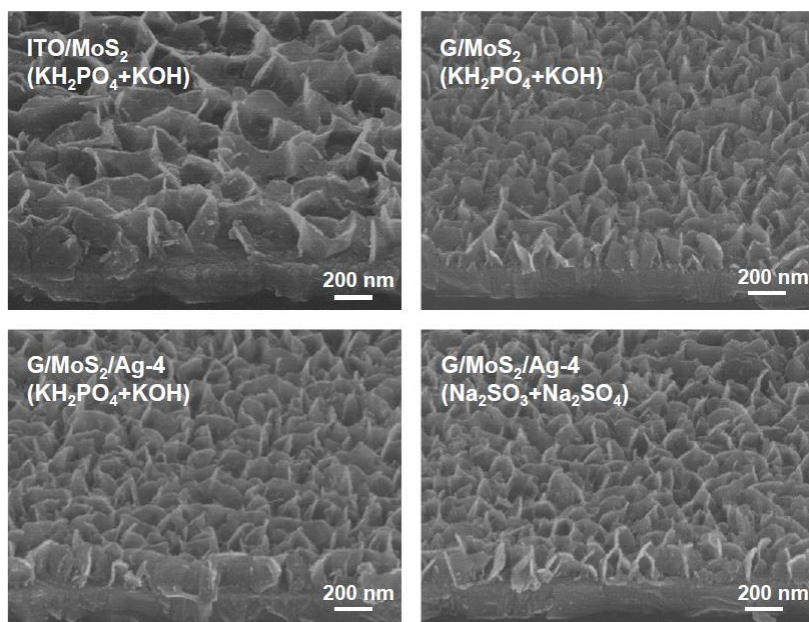


**Fig. S10** SEM images of ITO/MoS<sub>2</sub>, G/MoS<sub>2</sub>, and G/MoS<sub>2</sub>/Ag-4 after PEC measurement for 1 h

**Table S1**  $R_{ct}$  and  $R_s$  values of EIS analysis in the dark and under illumination

Samples	Dark		Illumination		$R_{ct}$ (dark)/ $R_{ct}$ (photo)
	$R_{ct}$ [ $\Omega$ ]	$R_s$ [ $\Omega$ ]	$R_{ct}$ [ $\Omega$ ]	$R_s$ [ $\Omega$ ]	
ITO/MoS <sub>2</sub>	4236	43.7	2766	45.5	1.53
G/MoS <sub>2</sub>	3264	40.1	1959	40.2	1.67
G/MoS <sub>2</sub> /Ag-2	2834	41.7	1780	41.7	1.59
G/MoS <sub>2</sub> /Ag-4	2572	40.2	1284	44.2	2.00
G/MoS <sub>2</sub> /Ag-8	3110	66.8	1947	48.3	1.60